*Small Molecule Therapeutics*

Molecular Cancer Therapeutics

# MTI-101 (Cyclized HYD1) Binds a CD44 Containing Complex and Induces Necrotic Cell Death in Multiple Myeloma

Anthony W. Gebhard[1,3], Priyesh Jain[2,4,5], Rajesh R. Nair[3,5], Michael F. Emmons[3], Raul F. Argilagos[3,5], John M. Koomen[3], Mark L. McLaughlin[2,4], and Lori A. Hazlehurst[3]

## Abstract

Our laboratory recently reported that treatment with the D-amino acid containing peptide HYD1 induces necrotic cell death in multiple myeloma cell lines. Because of the intriguing biological activity and promising *in vivo* activity of HYD1, we pursued strategies for increasing the therapeutic efficacy of the linear peptide. These efforts led to a cyclized peptidomimetic, MTI-101, with increased *in vitro* activity and robust *in vivo* activity as a single agent using two myeloma models that consider the bone marrow microenvironment. MTI-101 treatment similar to HYD1 induced reactive oxygen species, depleted ATP levels, and failed to activate caspase-3. Moreover, MTI-101 is cross-resistant in H929 cells selected for acquired resistance to HYD1. Here, we pursued an unbiased chemical biology approach using biotinylated peptide affinity purification and liquid chromatography/tandem mass spectrometry analysis to identify binding partners of MTI-101. Using this approach, CD44 was identified as a predominant binding partner. Reducing the expression of CD44 was sufficient to induce cell death in multiple myeloma cell lines, indicating that multiple myeloma cells require CD44 expression for survival. Ectopic expression of CD44s correlated with increased binding of the FAM-conjugated peptide. However, ectopic expression of CD44s was not sufficient to increase the sensitivity to MTI-101–induced cell death. Mechanistically, we show that MTI-101–induced cell death occurs via a Rip1-, Rip3-, or Drp1-dependent and -independent pathway. Finally, we show that MTI-101 has robust activity as a single agent in the SCID-Hu bone implant and 5TGM1 *in vivo* model of multiple myeloma. *Mol Cancer Ther; 12(11); 2446–58. ©2013 AACR.*

## Introduction

Multiple myeloma is a malignant cancer that results in the uncontrolled proliferation of plasma cells that aberrantly home to the bone marrow. The accumulation of multiple myeloma in the bone marrow eventually leads to uncoupling of bone remodeling, resulting in painful bone lesions (1). Although there are a multitude of treatments for multiple myeloma, minimal residual disease is thought to lead to the outgrowth of a drug-resistant population that renders multiple myeloma incurable (1–4). Therefore, it is imperative that novel therapies that target multiple myeloma in the context of the bone marrow microenvironment are developed. Experimental evidence indicates that homing of myeloma cells to the bone marrow is predominately driven by the chemokine SDF-1 and the cell adhesion molecules CD44 and VLA-4 integrin (5–7). In addition to contributing to homing, adhesion of myeloma cells via VLA-4 or CD44 can contribute to drug resistance (8–10). Thus, experimental and clinical evidence continues to support the development of therapeutic strategies for targeting pathways critical for regulation of homing to the bone marrow, as well as survival in the context of the bone marrow microenvironment.

Our laboratory has previously shown that the novel D-amino acid peptide HYD1 (kikmviswkg), discovered for blocking cell adhesion (11–13), also induces necrotic cell death as a single agent in multiple myeloma cells (14). More recently, we reported that the linear peptide shows increased potency in specimens obtained from relapsed multiple myeloma patients (15). We implicated the adhesion receptor α4-integrin as being partially involved in HYD1-induced cell death via shRNA-silencing strategies. However, reducing α4-integrin expression only demonstrated partial protection, indicating that other components of the HYD1 binding complex may be required for cell death (15).

To further characterize the entire binding complex of HYD1, we performed a total membrane binding assay using biotin-HYD1 in NCI-H929 and U266 multiple myeloma cells and NeutrAvidin beads to isolate HYD1 complexes for liquid chromatography/tandem mass spectrometry (LC/MS-MS) identification of bound

**Authors' Affiliations:** [1]Molecular Pharmacology and Physiology Program; [2]Department of Chemistry, University of South Florida; [3]Molecular Oncology Program; [4]Department of Drug Discovery, H. Lee Moffitt Cancer Center and Research Institute; and [5]Modulation Therapeutics Inc., Tampa, Florida

**Note:** Supplementary data for this article are available at Molecular Cancer Therapeutics Online (http://mct.aacrjournals.org/).

**Corresponding Author:** Lori A. Hazlehurst, Molecular Oncology Program, H. Lee Moffitt Cancer Center, Tampa, FL. Phone: 813-903-6807; Fax: 813-979-7265; E-mail: Lori.Hazlehurst@moffitt.org

**doi:** 10.1158/1535-7163.MCT-13-0310

proteins. The glycoprotein adhesion receptor CD44 was among the top proteins identified by LC/MS-MS. Given the abundance of literature implicating CD44 in caspase-independent and -dependent cell death, we thought that CD44 warranted further investigation (16–20). The predominant ligand for CD44 is the glycosaminoglycan hyaluronic acid. However, CD44 can also bind to other extracellular matrix components such as osteopontin, fibronectin, laminin, and collagen as well E-selectin (21). Paradoxically, CD44, depending on the cell context, can contribute to either survival or cell death. T cells derived from CD44-null mice are shown to be resistant to cell death induced by concanavalin A stimulation and T-cell receptor-induced cell death (22, 23). These data indicate that CD44 may be required for depletion of activated T cells. More recently, Ruffell and Johnson showed that activation of CD44 expressing Jurkat T cells with PMA sensitized these cells to HA-induced cell death (24). Of note, cell death was independent of activation of caspase-8; and could not be blocked by treatment with the pan-caspase inhibitor z-VAD-fmk. These data suggest that intracellular signaling and not expression may dictate CD44-mediated cell death. Similarly our data indicate that CD44 expression correlates with binding of HYD1 and a cyclized peptidomimetic derivative, referred to as MTI-101; however, ectopic expression of CD44s was not predictive for increased MTI-101-induced cell death. Together these data indicate that background cellular signaling or lateral signaling and not target expression may dictate sensitivity and selectivity of this class of compounds. In this study, our data suggest that the optimized analog MTI-101 is mechanistically similar to the linear HYD1 peptide and induces caspase-independent cell death. Reducing known mediators of necrosis including Drp1 protected U266 but not NCI-H929 cells from MTI-101-induced cell death. We postulate that necrotic cell death similar to mediators of apoptosis is likely driven by redundant pathways. MTI-101 shows robust *in vivo* activity as a single agent and our data continue to support further preclinical development of MTI-101 for the treatment of multiple myeloma.

## Materials and Methods

### Cell culture

NCI-H929, U266, and 8226 cell lines were purchased from American Type Culture Collection and maintained at 37°C and 5% $CO_2$. Cells were cultured in RPMI-1640 media (GIBCO; Life Technologies) and supplemented with 10% FBS (GIBCO). For NCI-H929 cells, 0.05 mmol/L 2-mercaptoethanol was added to culture media. 293FT cells were purchased from Invitrogen and grown in Iscove's Dulbecco's Modified Eagle's Medium (Cellgro) and supplemented with 10% FBS (GIBCO). Our cell lines are mycoplasm negative and $\kappa$ and $\lambda$ immunoglobulin expression levels are routinely determined. Myeloma cell lines were tested for secretion of $\kappa$ (NCI-H929) or $\lambda$ (RPMI-8226 and U266) levels by ELISA and mycoplasm every 6 months.

### Peptides, reagents, and antibodies

HYD1, biotin-HYD1, and 5(6)-FAM-HYD1 were synthesized by Bachem. MTI-101 and biotin-MTI-101 were synthesized by Drs. McLaughlin and Jain. The method of synthesis for MTI-101 is as follows; *p*-Nitrophenyl Wang Resin (0.69 mmol/g, 100 mg) was swollen in dichloromethane (DCM) for 15 minutes. $N^{\alpha}$- Fmoc-Lys-OAllyl. Trifluoroacetic acid (TFA; 4 equivalents) solution in DCM containing N,N-diisopropylethylamine (DIEA; 8 equivalents) was added to the resin in a peptide reaction vessel for 3 hours. The process is repeated twice to ensure maximum loading of the Fmoc amino acid on the resin. $N^{\alpha}$- Fmoc-Lys-OAllyl. TFA salt was prepared by deprotection of $N^{\alpha}$- Fmoc-Lys(Boc)-OAllyl using 95% TFA in DCM at 0°C. Fmoc quantification of resin indicated a loading of 0.65 mmol/g of resin. The linear protected peptide was then synthesized using standard Fmoc solid phase strategy. For each coupling step, 2 equivalents of symmetrical anhydride of Fmoc-amino acid (concentration of 220 mmol/L) in DCM were added to the reactor. Each coupling reaction was carried out for 1 hour followed by N-methyl-2-pyrrolidone (NMP; 3 × 2 mL) and DCM (4 × 2 mL) washes. Fmoc deprotection was done using 20% piperidine/2% DBU in NMP (3 mL) for 10 minutes. Then the amino acids used for peptide synthesis were coupled in the following order: Fmoc-Leu-OH, Fmoc-Lys(Boc)-OH, Linker $T_3$, Fmoc-Trp(Boc)-OH, Fmoc-Ala-OH, Fmoc-Val-OH, Fmoc-Val-OH, Fmoc-Nle-OH, Linker $T_1$, Fmoc-Lys(Boc)-OH, Fmoc-Leu-OH. After synthesis of the protected linear peptide, the Fmoc group from last amino acid was cleaved by 20% piperidine/2% DBU in DMF. The C-terminal allyl group was then removed using 0.2 mol% $Pd(PPh_3)_4$ dissolved in $CHCl_3$-AcOH-NMM (37:2:1; 3 mL) for 1 hour. The allyl cleavage procedure was repeated again to ensure complete cleavage. The resulting side chain anchored peptide acid resin was then washed with DCM, NMP, MeOH, DCM, and dried. After allyl deprotection on resin, cyclization of linear peptide was carried out by treating peptide side chain anchored peptide acid resin with 4 equivalents of HCTU (220 mmol/L) in NMP and 8 equivalents of DIEA for 1 hour. The peptidyl resin was then washed with NMP (3 × 2 mL) and DCM (4 × 2 mL). The peptide was deprotected from the resin using cleavage cocktail of TFA/phenol/$H_2O$/EDT/TIS (82.5:5:5:5:2.5) solution (4 mL) at room temperature for 30 minutes. The reaction mixture was concentrated and the thick viscous liquid was triturated twice with 10 mL of cold diethyl ether. The reaction contents were centrifuged to give crude cyclic MTI-101 peptidomimetic. The crude peptidomimetic was dissolved in a solution of 0.1% TFA in $H_2O$ and freeze-dried to give 85 mg of crude MTI-101. Crude MTI-101 was then purified using semipreparative reverse phase high-performance liquid chromatography (HPLC; 5 μmol/L particle size C8 AAPPTEC spirit column, 25 × 2.12 cm) with eluents: A = 0.1% TFA in $H_2O$, B = 0.1% TFA in $CH_3$ CN. The purification was carried out using a gradient of 10% B for 10 minutes and then 29% to 32% B more than 60

minutes with a flow rate 20 mL/min using 222 nm UV detection. All peaks with retention times expected for peptides were collected and lyophilized. The purified MTI-101 was analyzed using similar analytical HPLC conditions and found to have >95% purity. Biotinylated MTI-101 peptide was synthesized on Rink amide resin using Fmoc solid phase peptide synthesis strategy. The linear peptide was synthesized by first attaching the γ-side chain carboxyl group of Fmoc-Asp-OAllyl to trifunctional linker on the resin. The linear peptide was then cyclized on resin, followed by attachment of biotin to 6-amino hexanoic acid on the trifunctional linker to give protected biotinylated cyclic peptide MTI-101. Biotinylated MTI-101 was then subsequently cleaved from the resin using TFA/TIS/$H_2O$ (95:2.5:2.5). The crude peptide was then lyophilized and purified by reverse phase column chromatography to greater than 94% purity. TO-PRO-3 iodide and CellROX Green Reagent were purchased from Invitrogen. Mdivi-1 and *tert*-butyl hydroperoxide were purchased from Sigma Aldrich. Recombinant soluble Killer Trail was purchased from Alexis Biosciences. Anti-CD44 (clone 156-3C11), anti-GAPDH (clone 14C10), anti-RIP1, anti-pDrp1 (Ser637), anti-Drp1 (clone D6C7), anti-pERK (T202/Y204), anti-Erk1/2, and anti-Basigin were purchased from Cell Signaling Technology. The anti-Rip3 and anti-Syndecan-1 were purchased from Abcam, and the anti-Pyk2/Cak β was purchased from BD Pharmigen. The anti-$IgG_{2a}$ mouse was purchased from BD Biosciences, anti-mouse immunoglobulin/FITC goat F(ab′)2 was purchased from Dako, and anti-rabbit HRP-conjugated and anti-mouse HRP-conjugated were purchased from Jackson ImmunoResearch Laboratories.

### Cell death analysis

Cells were plated at a density of $4 \times 10^5$ cells/mL and treated with varying concentrations of peptide for 24 hours. Cells were then washed with PBS and incubated with 2 nmol/L TO-PRO-3 iodide and immediately analyzed for fluorescence intensity using the FACSCalibur flow cytometer (BD Biosciences).

### Cleaved caspase-3 activity assay

Treated and control NCI-H929 and U266 cells were plated at a density of $4 \times 10^5$ cells/mL before being assessed for cleaved caspase-3 levels using the caspase-3 active form mAb FITC kit (BD Pharmigen), as per the manufacturer's instructions. Samples were analyzed using the FACScan flow cytometer (BD Biosciences).

### Biotin-HYD1 complex capture from total membrane lysate

The capture of the biotin-HYD1 binding complex was performed as previously described (15). Briefly, $1.2 \times 10^8$ NCI-H929 or U266 cells were incubated for 30 minutes on ice in AP buffer (25 mm HEPES pH 8.0, 100 mmol/L KCl, 1 mmol/L MgCl, 1 mmol/L CaCl, 20% glycerol, 1 mmol/L PMSF, and 1 μg/mL leupeptin and aprotinin) and Dounce homogenized. Total cell membrane lysate was obtained through centrifugation and quantified by BCA kit (Pierce); 500 μg of biotin or biotin-HYD1 was incubated with 30 μL of NeutrAvidin beads (Pierce) for 1 hour at room temperature, followed by 2 washes in AP buffer. Membrane lysate (300 μg) was added to beads, and volume was adjusted to 500 μL and incubated overnight at 4°C. After 3 washes in AP buffer containing 0.2% NP-40, beads were boiled in Laemmli loading buffer and eluted proteins were fractionated by SDS-PAGE.

### LC/MS-MS analysis of biotin-HYD1 binding complex

Proteins were digested in-gel with trypsin; the resulting proteolytic peptides were analyzed. Samples were resolved by SDS-PAGE, trypsin digested, and analyzed by LC/MS-MS and identified using Mascot and Sequest searches against human entries in the UniProt databases. Scaffold (v.3 Proteome Software) was used for data mining of proteins identified in the biotin-HYD1 binding complex.

### ATP measurement

NCI-H929 or U226 cells were treated (400,000 cells/mL) for 1 hour at 5 and 10 μmol/L, respectively. Live and dead cells were then counted and subsequently lysed in a buffer containing 40 mM Tris, 20 mM acetic acid, and 1 mM EDTA pH 7.4 (TAE) buffer containing 50 μL of 1% trichloroacetic acid. Cells were lysed by 3 snap freeze–thaw cycles and then resuspended in 450 μL of TAE buffer. The lysate was centrifuged at $2{,}000 \times g$ for 15 minutes, and supernatant was transferred to Eppendorf tubes. ATP was measured immediately using the ENLITEN ATP assay kit (Promega), and bioluminescence was measured and normalized to cell number.

### siRNA transfection

Transfection of NCI-H929 and U266 cells was performed as previously described (14). Briefly, $2 \times 10^6$ cells were added to 200 μL of cytomix buffer (in mmol/L: 120 KCl, 0.015 $CaCl_2$, 10 $K_2HPO_4/KH_2PO_4$, 25 HEPES, 2 EGTA, 5 $MgCl_2$, 2 ATP, 5 gluthathione, and 1.25% DMSO; pH 7.6). Ten microliters of a 20 μmol/L stock of SMARTpool siRNA directed at Rip1 (Dharmacon), Rip3 (IDT), Drp1 (Dharmacon), basigin (Dharmacon), syndecan-1 (Dharmacon), or nonsilencing (Dharmacon) was added to the buffer. The mixture was placed in a 2-mm cuvette and electroporation was done at 140V/975 μF. After transfection, cells were incubated in the buffer for 15 minutes in a 37°C incubator before being transferred into a 25-mL flask containing 10 mL of fresh media. Cells were incubated for 72 hours before treatment with MTI-101. For CD44, 20 μL of a 20 μmol/L stock of SMARTpool siRNA (Dharmacon) was used, and cells were electroporated a second time at 24 hours to achieve efficient reduction in surface expression.

### Recombinant CD44 ELISA binding assay

NeutrAvidin (Pierce) plates were prepared by adding 100 μL of 50 μg/mL or biotin or biotin-HYD1 in binding

buffer (in mmol/L: 0.5 KCl, 0.3 $KH_2PO_4$, 27.6 NaCl, 1,6 $Na_2HPO_4$; pH 7.4) for 2 hours at room temperature. Full-length recombinant human CD44 (Abnova) was then added to the 96-well plates at increasing concentrations and allowed to incubate for 2 hours in 500 μL of buffer A (25 mmol/L Tris, 150 mmol/L NaCl, 1.0% bovine serum albumin, 0.05% Tween 20, pH 7.25%). Bovine serum albumin was added to control for nonspecific binding. A 1:500 dilution of primary CD44 antibody was added to each well and incubated for an additional hour, wells were washed, and a 1:10,000 dilution (buffer A) of the secondary antibody was added to each well for an additional 30 minutes at room temperature. Wells were washed again, and 100 μL of Pico chemiluminescent substrate (Pierce) was added to each well. After addition of substrate, plates were read on a Victor chemiluminescence plate reader.

### CD44 overexpression in RPMI-8226 cells

Stable RPMI-8226 cells overexpressing CD44s were generated by infection with retrovirus and puromycin selection. Briefly, 293FT cells were grown to 90% confluence in 100-mm Petri dishes and then transfected with the pBabe-puro CD44s retroviral vector (Addgene plasmid 19127) synthesized by the Weinberg lab or a scrambled retroviral CD44 shRNA (Origene) using the pVPack system (Clontech). RPMI-8226 cells were then infected with the retrovirus for 72 hours, and 1 μg/mL puromycin (Invitrogen) was added to allow for the selection of a stable population of cells.

### 5(6)-FAM-HYD1 binding assay

RPMI-8226 vector control and CD44s overexpressing cells were plated at a density of $4 \times 10^5$ cells/mL and incubated with 6.25 μg/mL 5(6)-FAM or 5(6)-FAM-HYD1 for 15 minutes on ice. Cells were then washed 3 times with cold PBS, with fluorescence immediately measured (FACScan flow cytometer, BD Biosciences).

### Immunoprecipitation

After treatment, cells were washed in cold PBS and lysed on ice with IP buffer (1% Triton X-100, 150 mmol/L NaCl, 10 mmol/L Tris pH 7.4, 1 mmol/L EDTA, 1 mmol/L EGTA, pH 8.0, 0.2 mmol/L sodium orthovanadate, 0.5% IGEPAL CA-630, and protease inhibitor cocktail), and 500 μg of cell lysate was precleared with 50 μL A/G beads (Pierce) for 30 minutes before being incubated with 5 μg anti-CD44 (156-3C11) overnight at 4°C. After incubation, lysates were incubated with 30 μL A/G beads for 1 hour and washed 3 times with IP buffer. Samples were then put in 2× Laemmli buffer and analyzed by Western blotting.

### SCID-Hu model

The SCID-Hu model was performed as previously described (14). Briefly, SCID/beige mice 4 to 6 weeks old were purchased from Taconic. Fetal tissue (18–23 weeks) was obtained from Advance Bioscience Resource in compliance with state and federal regulations. One bone were surgically implanted in the mammary fat pad of 6- to 8-week female SCID mice. After 6 weeks of bone engraftment, 50,000 H929 cells were injected directly into the bone and tumor was allowed to engraft for 4 weeks. At 28 days, baseline tumor burden was quantified in the sera using a κ ELISA kit (Bethyl), and mice were randomized into treatment groups (10 mice per group). Mice were treated intraperitoneally with 8 mg/kg MTI-101 or PBS daily for 21 days. To assess tumor burden as a function of time, κ levels in the sera were measured weekly.

### 5TGM1 myeloma mouse model

A total of $1 \times 10^6$ 5TGM1 cells were injected into 6–8 week old C57BL/KaLwRijHsd mice via tail vein. At day 10, mice were treated with agents at the indicated doses 3 times a week for 3 weeks. All drugs were administered intraperitoneally. IgG2B serum levels were measured by ELISA once a week for 4 weeks per the manufacturer's instructions (Bethyl). Mice were monitored daily for survival with all remaining mice euthanized at day 100. We found that the maximum tolerated dose was 50 mg/kg as we observed early deaths in this cohort (2 of 10 animals).

## Results

### MTI-101 (cyclized HYD1) is more potent *in vitro* compared with the parent HYD1 compound, is cross-resistant in the H929-60 cell line, and induces caspase-3–independent cell death, ATP depletion, and ROS production in NCI-H929 and U266 cells

HYD1 was previously shown to induce caspase-independent necrotic cell death, ATP depletion, mitochondrial membrane potential dysfunction, and reactive oxygen species (ROS) production in NCI-H929, U266, and RPMI-8226 cell lines (14). In this study, we took the minimally active truncated core region of HYD1 (mvisw; Fig. 1A) and cyclized that peptide using a β turn promoter scaffold backbone. The initial sequence inserted was mvisw that was subsequently optimized in the L-configuration. The solubility of mvisw was very poor but the 3 lysines on the nonrecognition strand render MTI-101 water soluble. Alanine scanning of the core sequence constrained in the β turn promoter was used to optimize the sequence. In this report, the most potent analog (MTI-101) contained the optimized sequence NLeVVAW comprised of all L-amino acid peptides within the β turn promoter scaffold backbone and was used for all subsequent studies (Fig. 1B). Survival curves were generated comparing HYD1 with MTI-101 in NCI-H929 cell line, with $IC_{50}$ values of 63.9 μmol/L ± 6.0 and 8.38 μmol/L ± 0.9, respectively (Fig. 1C). We also observed an increase in potency of MTI-101 when compared to HYD1 in U266 cell line, with $IC_{50}$ values of 89.03 μmol/L ± 18.6 for HYD1 and 22.1 μmol/L ± 4.25 for MTI-101 (Supplementary Fig. S1A). In addition, we observed that the acquired HYD1-resistant cell line H929-60 that was developed in our laboratory was cross-

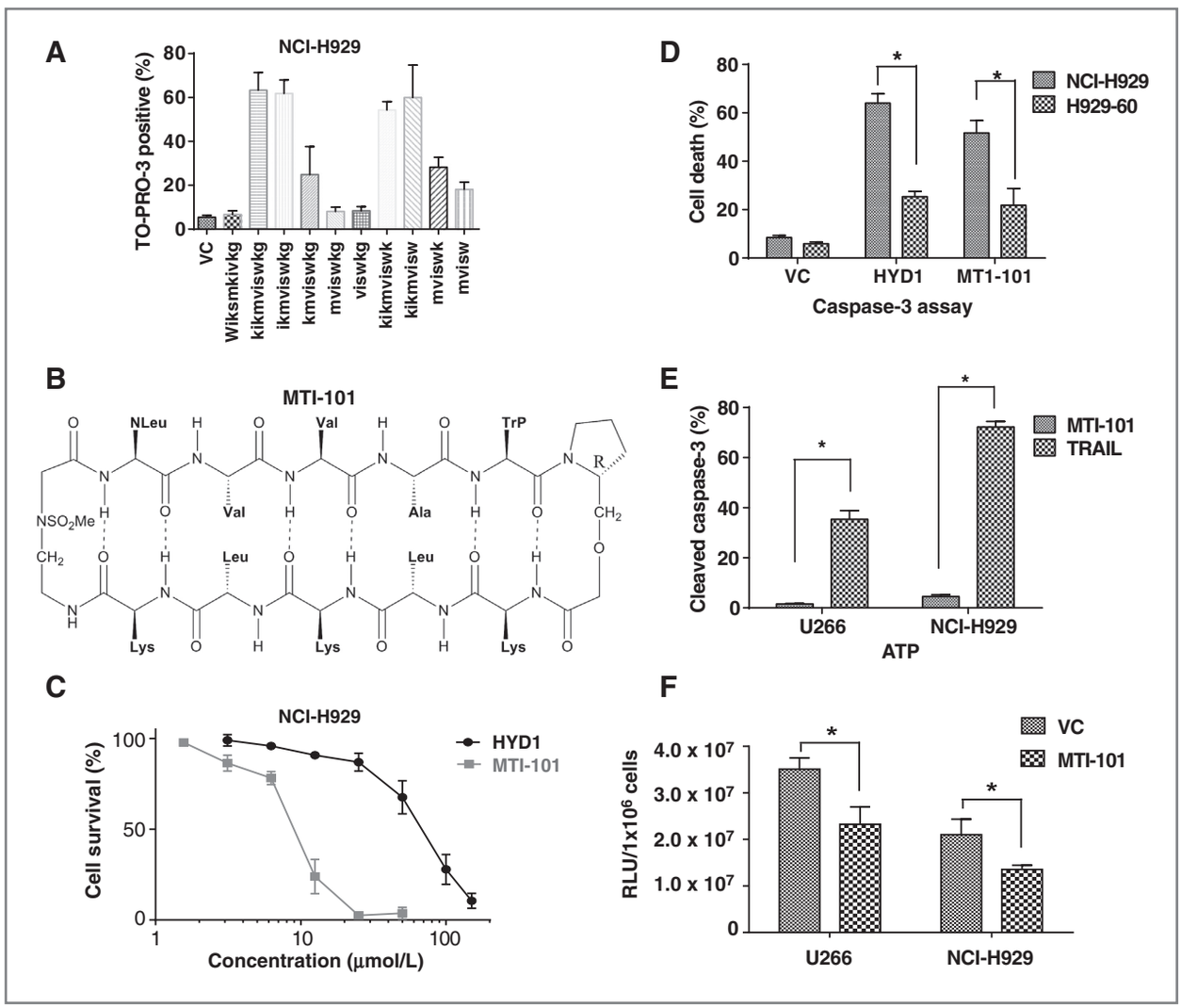


Figure 1. MTI-101 is more potent *in vitro* compared with HYD1, is cross-resistant in H929-60 cell line, results in caspase-independent cell death, and ATP depletion in NCI-H929 and U266 multiple myeloma cells. A, truncation studies to determine minimal active core mvisw. B, the structure of the most potent analog, MTI-101. The initial sequence inserted was mvisw that was subsequently optimized in the L-configuration. The solubility of mvisw was very poor, but the 3 lysines on the nonrecognition strand render MTI-101 water soluble. The optimized sequence of MTI-101 containing all L-amino acid peptides within the β turn promoter scaffold backbone is NLeVVAW and was used for all subsequent studies. C, a direct comparison of HYD1 and MTI-101 was performed in NCI-H929 cells treated for 24 hours and cell death was determined by FACS analysis. Cell survival curves were generated and $IC_{50}$ values were calculated; 63.9 μmol/L ± 6.0 for HYD1 and 8.38 μmol/L ± 0.9 for MTI-101. Cell death was measured by TO-PRO-3 staining and FACS analysis. D, MTI-101 is cross-resistant in the HYD1 acquired resistant H929-60 cell line. NCI-H929 and H929 cells were treated for 24 hours with 75 μmol/L HYD1 and 3 μmol/L MTI-101. E, NCI-H929 and U266 cells were treated with 5 and 10 μmol/L of MTI-101, respectively, for 24 hours and then caspase-3 activity was measured. Treatment with TRAIL was used as a positive control for cleaved caspase-3 activity. F, NCI-H929 and U266 cells were treated for 1 hour with 5 and 10 μmol/L MTI-101 and total cellular levels of ATP were measured (RLU, relative luminescence untis). Experiments were run in triplicate and repeated 3 times. Statistical significance was determined by ANOVA, *, $P \leq 0.05$.

resistant to MTI-101 (Fig. 1D). As with the previous study describing the mechanism of linear HYD1, we were interested in delineating the mechanism by which MTI-101 treatment resulted in cell death in myeloma cells. When NCI-H929 and U266 cells were treated with 5 and 10 μmol/L MTI-101, respectively, we did not detect cleaved caspase-3 (Fig. 1E). Treatment with recombinant soluble Killer Trail was used as a positive control. Similar to HYD1, we observed a statistically significant decrease in ATP levels in NCI-H929 and U266 cells upon treatment with 5 and 10 μmol/L MTI-101 (Fig. 1F). Furthermore, treatment with MTI-101 resulted in a statistically significant increase of ROS production (Supplementary Fig. S1B). Taken together, these data suggest that MTI-101 may be mechanistically similar to the linear peptide HYD1 as evidenced by disrupted mitochondrial function without activation of caspase-3.

### CD44 binds to HYD1 and is found in the biotin-HYD1 and biotin-MTI-101 binding complex in NCI-H929 and U266 cells

Previously, we showed α4-integrin as being part of the HYD1 binding complex (15). To this end, we saw partial, but not complete, protection from HYD1-induced cell death when α4-integrin expression was reduced, thereby indicating other proteins must be involved in mediating cell death. Using an unbiased chemical biology approach, we sought to identify the biotin-HYD1 and biotin-MTI-101 binding complex. Biotin was conjugated to the N-terminal lysine residue of HYD1 and this chemical probe (biotin-HYD1) was initially validated as retaining biological activity *in vitro* (Supplementary Fig. S1C). Given that our previous study showed HYD1 binding at the cell surface (15), we isolated total membrane fractions from NCI-H929 and U266 cells and incubated these fractions with biotin-HYD1. Complexes were then resolved by SDS-PAGE before LC/MS-MS protein identification. These data were then mined using the Scaffold 3 Proteome software, and adhesion receptors with their respective number of peptides were identified from the HYD1 binding complex (Supplementary Fig. S2). The glycoprotein receptor CD44 was identified in both myeloma cell lines. CD44 is known to associate with α4-integrin and is critical for homing and extravasation (25). Further validation of CD44 being present in the biotin-HYD1 and biotin-MTI-101 binding complex was confirmed using Western blot analysis (Fig. 2A). Based on previous reports implicating CD44 in both caspase-independent and -dependent cell death (16–20), we postulated that CD44 may be the initial binding target of HYD1 and MTI-101 and is required for initiating the cell death cascade induced by treatment in myeloma cells. To investigate whether CD44 binds directly to HYD1, we coated 96-well NeutrAvidin plates with biotin-HYD1 and incubated the plates with full-length recombinant human CD44. We observed a concentration-dependent increase in binding of recombinant CD44

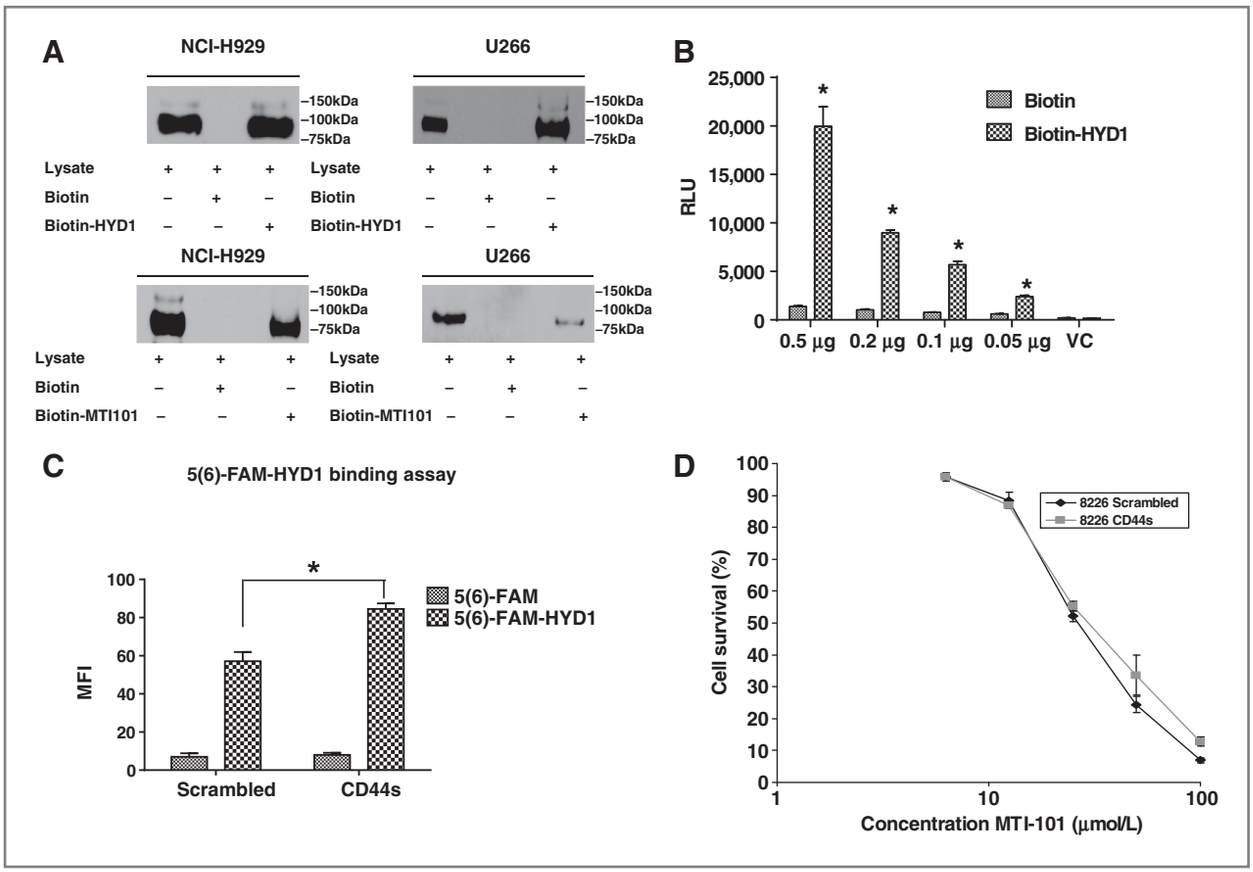


Figure 2. CD44 binds to HYD1 and is affinity purified in the biotin-HYD1 and biotin-MTI-101 binding complexes from NCI-H929 and U266 multiple myeloma cells. A, confirmation by Western blot analysis. Membrane lysate (150 μg) was incubated with 500 μg of biotin, biotin-HYD1, or biotin-MTI-101 bound to NeutrAvidin beads. Beads containing complexes were incubated overnight, washed, and proteins separated by SDS-PAGE, and probed for CD44. B, ELISA-based binding assay confirms that biotin-HYD1 binds to full length recombinant human CD44 in a concentration-dependent manner (RLU, relative luminescence units). Biotin was bound to NeutrAvidin-coated wells to control for nonspecific binding. C, overexpression of CD44s in RPMI-8226 multiple myeloma cells resulted in increased binding of fluorescently labeled HYD1. Median fluorescence intensity (MFI) and bound FAM-HYD1 were detected by FACS analysis. D, overexpression of CD44s did not result in increased sensitivity to MTI-101. Experiments were run in triplicate and repeated 3 times. Statistical significance was determined using ANOVA, *, $P \leq 0.05$.

(Fig. 2B). To investigate whether overexpression of CD44 in multiple myeloma cells would increase HYD1 binding, we used the RPMI-8226 cell line as RPMI-8266 cells had the lowest basal level of CD44 among the tested myeloma cell lines (data not shown). Retroviral infection of CD44s was used to overexpress CD44 in 8226 cells, and expression was confirmed by Western blot (Supplementary Fig. S3A). A HA adhesion assay was performed to confirm that functional CD44s was being expressed (Supplementary Fig. S3B). Although we observed an increase in binding to HA, this increase was only 2.5-fold whereas expression was increased more drastically. As shown in Fig. 2C, there was a 1.5-fold increase ($P < 0.05$, ANOVA Bonferroni *post hoc*) of 5(6)-FAM-HYD1 binding in the RPMI-8226 CD44s overexpressing cells compared with vector only cells. Finally, we investigated whether overexpression of CD44s was sufficient to increase the sensitivity to MTI-101–induced cell death. As shown in Fig. 2D, we did not observe a statistically significant change in cell death between the CD44s-overexpressing cells and the vector control. These data indicate that CD44s expression correlates with binding of 5(6)-FAM-HYD1 but not cell death. In addition, although these data indicate that CD44s expression is not rate limiting with respect to cell death, these results do not rule out the potential role of (i) intracellular signaling analogous to an activated T cell dictates sensitivity to ligand induced cell death, (ii) lateral or downstream signaling components such as α4-integrin, or (iii) expression of CD44 splice variant as being rate limiting for MTI-101–induced cell death. We are currently pursuing the downstream binding partners of CD44, which may be rate limiting for mediating MTI-101 induced cell death.

### Reduction of CD44 cell surface expression results in the activation of cleaved caspase-3 in NCI-H929 and U266 cells

To further address the role of CD44 in MTI-101–induced cell death in myeloma, we reduced cell surface expression targeting of all isoforms of CD44 in

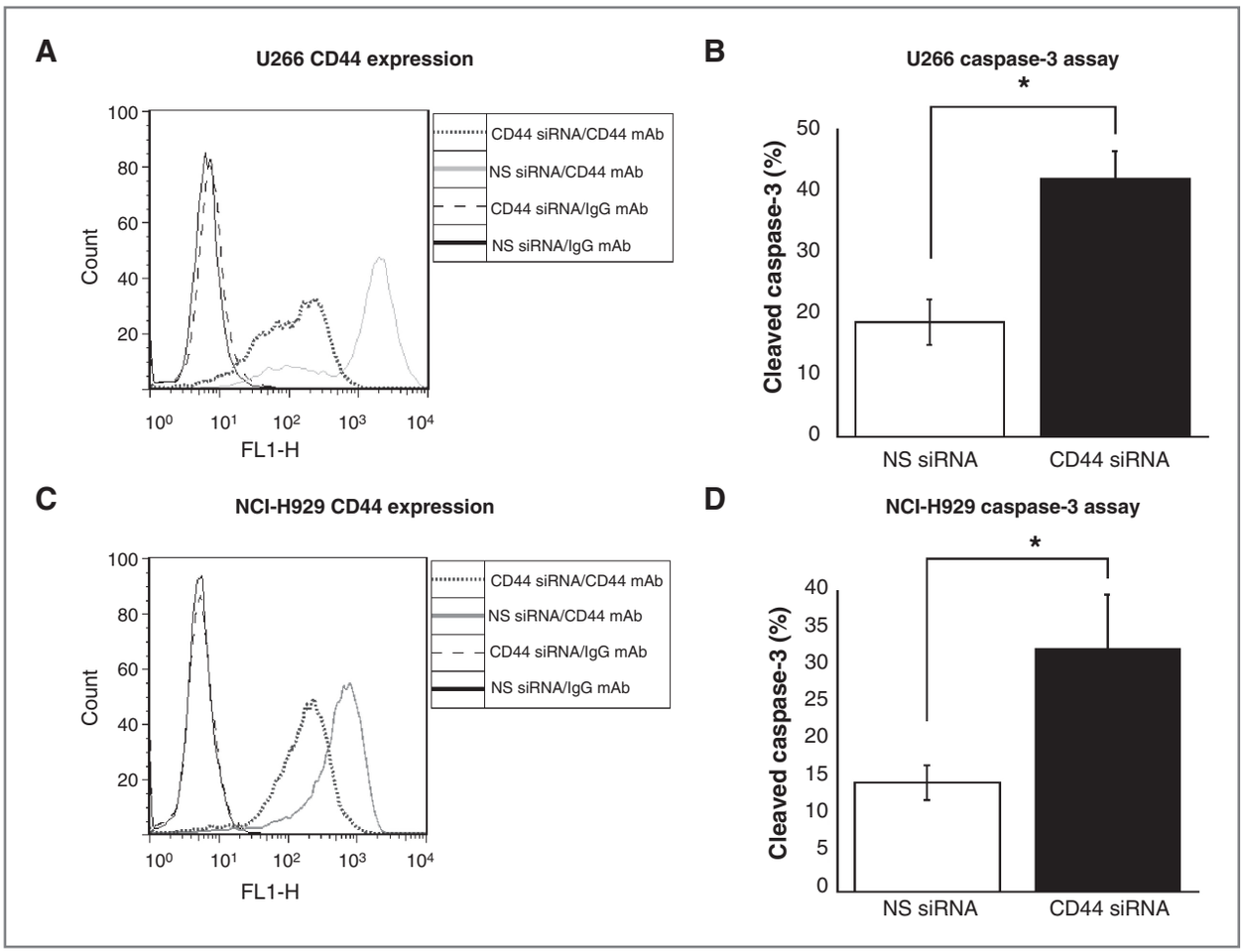


Figure 3. Reduction in CD44 expression induces cell death in U266 and NCI-H929, as determined through cleaved caspase-3 activation. A and C, CD44 expression determined by FACS analysis in U266 and NCI-H929 multiple myeloma cells. B and D, reduction of CD44 surface expression in U266 and NCI-H929 multiple myeloma cells results in the activation of cleaved caspase-3 (NS, nonsilencing). Experiments were run in triplicate and repeated 3 times. Statistical significance was determined using Student *t* test, *, $P \leq 0.05$.

NCI-H929 and U266 cell lines. Optimal reduction in CD44 expression was achieved 72 hours after siRNA transfection (Fig. 3A and C). Interestingly, we observed that, when CD44 expression was reduced, both cell lines seemed to be less viable compared with the nonsilencing control cells. To assess which cell death pathway was involved in this observation, we used a caspase-3 antibody, which only recognizes the active form of caspase-3. As shown in Fig. 3B and 3D, reduction in cell surface expression of CD44 resulted in a significant increase in cleaved caspase-3 versus that shown in nonsilencing control cells. These data suggest that CD44 is required for survival in myeloma cell lines, validate CD44 as a potential target for the treatment of MM, and indicate that CD44 may be a key regulator of both ligand induced necrotic cell death and inhibitor of apoptotic cell death. To examine other members of the binding complex, we reduced the expression of syndecan-1 and basigin. Reducing the expression of basigin or syndecan-1 failed to confer resistance to MTI-101–induced cell death (Supplementary Figs. S4 and S5).

### MTI-101 induces CD44-associated agonistic signaling in NCI-H929 and U266 cells

CD44 has been shown to associate with focal adhesions and a number of cell signaling pathways (26–28). Furthermore, we previously showed that HYD1 induces autophagy, which protects myeloma cells against death (14). To examine whether MTI-101 treatment would modulate the interaction between CD44 and its associated proteins, we pretreated NCI-H929 and U266 cells with MTI-101 and performed a CD44 immunoprecipitation assay. As shown in Fig. 4A and B, there was an increased association with the focal adhesion tyrosine kinase protein Pyk2 immediately following MTI-101 treatment in both myeloma cell lines. We also observed a transient activation of Erk/Map kinase pathway upon MTI-101 treatment in NCI-H929 and a more sustained activation in U266 cells (Fig. 4C and D). Taken together, these data indicate that MTI-101 induces agonistic CD44-associated signaling as evidenced with association of CD44 with Pyk2 and activation of the Erk pathway. Furthermore, the activation of the Erk pathway and Pyk2 may lead to the rationale design of combination strategies for increasing the efficacy of this novel class of compounds.

### Reduction in Rip1, Rip3, and Drp1 expression results in modest increase in survival of U266 cells upon MTI-101 treatment

Recently, numerous reports have indicated that cells can initiate an apoptotic-like programmed form of necrosis called necroptosis. Critical mediators of necrosis include the serine/threonine kinases Rip1 and Rip3 and the GTPase, Drp1. Drp1 is critical driver of mitochondria fission and activity of the GTPase is negatively regulated by phosphorylation on Ser 637 (for review, see refs. 29 and 30). Using siRNA targeting Rip1, Rip3, or Drp1, we achieved efficient reduction in protein expression in U266 cells 72 hours after transfection. Following siRNA transfection cells were treated with 10 μmol/L MTI-101 for 6 hours before cell death was quantified via TO-PRO-3 iodide staining and FACS analysis. Our results showed a modest, but significant, increase in cell survival upon MTI-101 treatment and reduced expression in each of the respective proteins involved in necroptosis in U266 cells (Fig. 5). To investigate pharmacological inhibition of the necroptotic pathway, cells were pretreated with 100 μmol/L of the Drp1 inhibitor mdivi-1 (31) for 1 hour before treatment with 10 μmol/L MTI-101 for 6 hours, with cell death quantified via TO-PRO-3 iodide staining and FACS analysis. Our results again showed a modest but significant increase in cell survival upon pretreatment with mdivi-1. We also observed a modest decrease in phosphorylated Drp1 levels in U266 cells upon MTI-101

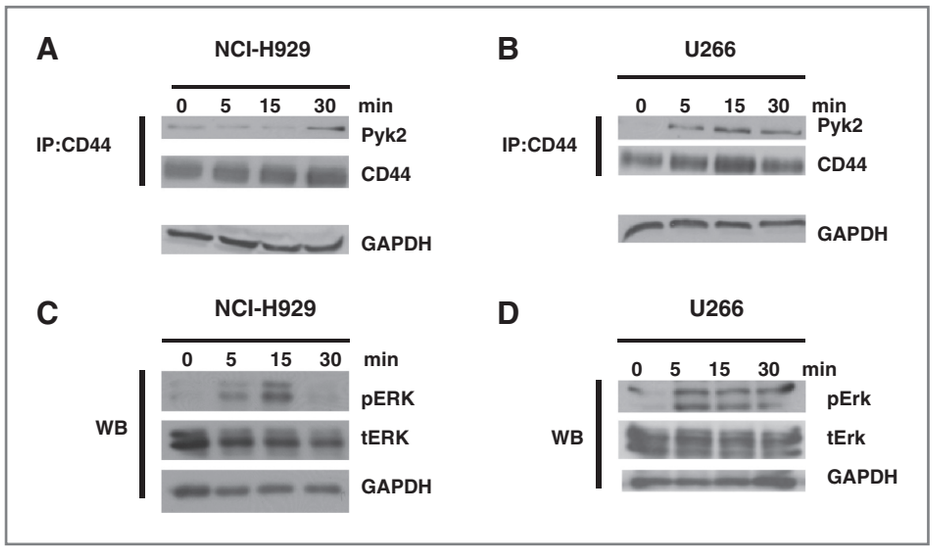


Figure 4. MTI-101 treatment induces transient phospho-Erk1/2 and CD44-associated Pyk2 complex in NCI-H929 and U266 multiple myeloma cells. A and B, CD44 immunoprecipation was performed after MTI-101 treatment in NCI-H929 and U266 cells and probed for Pyk2 and CD44. GAPDH levels in the total lysaste were used as a loading control. C and D, NCI-H929 and U266 cells were treated with 5 and 10 μmol/L MTI-101, respectively, for various time points before whole cell lysis in RIPA buffer and probed for pErk (T202/Y204) and total Erk. Experiments were repeated 3 times and shown is a representative Western blot.

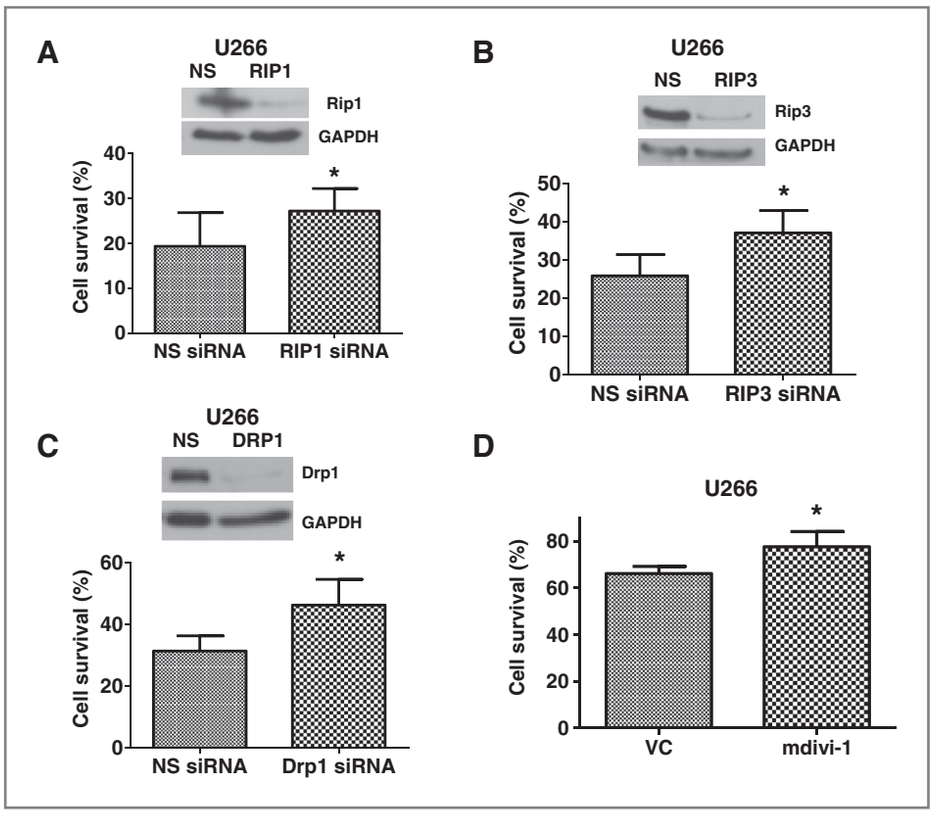


Figure 5. Reduction in RIP1/RIP3 and DRP1 expression results in modest increase in survival in U266 multiple myeloma cell line upon MTI-101 treatment. U266 cells were incubated with siRNA targeting RIP1 (A), RIP3 (B), and DRP1 (C) for 72 hours before treatment with 10 μmol/L MTI-101 for 6 hours, and cell death was determined by FACS analysis. A–C, a modest, but statistically significant increase in survival was observed in U266 cells. D, U266 cells were pretreated with 100 μmol/L mdivi-1 for 1 hour before treatment with 10 μmol/L MTI-101 for 6 hours, and cell death was determined by FACS analysis. NS, nonsilencing. Experiments were run in triplicate and repeated 3 times. Statistical significance was determined using Student *t* test, *, $P \leq 0.05$.

treatment (Supplementary Fig. S6A), suggesting that MTI-101 induces activation of Drp1. During necroptosis activation of the phosphatase, Pgam5 is required for dephosphorylation and subsequent activation of the GTPase Drp1, leading to mitochondrial fission and necrosis (32, 33). Together, these data indicate that Rip1/Drp1-dependent necroptosis is partially involved in MTI-101–induced cell death in the U266 myeloma cell line.

## MTI-101 necrotic cell death is Drp1 independent in NCI-H929 cells

In NCI-H929 cells, we did not observe a statistically significant difference in cell survival upon MTI-101 treatment when Drp1 expression levels were reduced using siRNA (Fig. 6A) and mdivi-1 pretreatment failed to be protective against MTI-101–induced cell death (Supplementary Fig. S6C). These results were consistent with no change in the levels of pDrp1 following MTI-101 treatment (Supplementary Fig. S6B). Furthermore, we did not observe any protection against MTI-101 when either Rip1 or Rip3 expression levels were reduced (Supplementary Fig. S6D and S6E). Finally, reducing the expression of Rip3 did not switch the mode of cell death to apoptosis in either U226 or NCI-H929 cells (Supplementary Fig. S6F). These data indicate that MTI-101–induced cell death is Rip1/Rip3 and Drp1 independent in NCI-H929 cells. In summary, we postulate that MTI-101 induces necrotic cell death via redundant pathways and inhibiting the Rip1/Rip3/Drp1-induced necrosis will not be sufficient to block MTI-101–induced cell death.

## MTI-101 inhibits myeloma tumor growth *in vivo*

We used the SCID-Hu and 5TGM1 *in vivo* myeloma mouse models to determine if MTI-101 was an efficacious antitumor agent. The SCID-Hu myeloma mouse model entails engrafting cadavered fetal bone into the mammary mouse pad. Importantly, the SCID-Hu model considers drug response in the confines of the bone marrow microenvironment without systemic disease confounding interpretation of drug response (34, 35). Thus, the SCID-Hu model is ideal for evaluating preclinical drugs for the treatment of myeloma. As shown in Fig. 6B, serum $\kappa$ levels were significantly decreased in the MTI-101 treatment group versus controls (ANOVA $P < 0.05$). During these studies, at the doses used no overt signs of toxicity were noted. The 5TGM1 mouse myeloma model entails engrafted 5TGM1 cells into C57BL/KaLwRijHsd mice via a tail vein injection. At day 10, mice were treated with agents 3 times a week for 3 weeks. Mice were monitored daily for survival with all remaining mice euthanized at day 100 after treatment. As shown in Fig. 6C, MTI-101 given at doses of 10 and 25 mg/kg 3 times weekly demonstrated a significant increase in survival compared to control animals ($P = 0.02$ at 10 mg/kg and $P = 0.002$ at 25 mg/kg Mantel–Cox test). In addition, serum $\kappa$ levels were significantly decreased (ANOVA $P < 0.05$) in the MTI-101 and bortezomib treatment groups versus

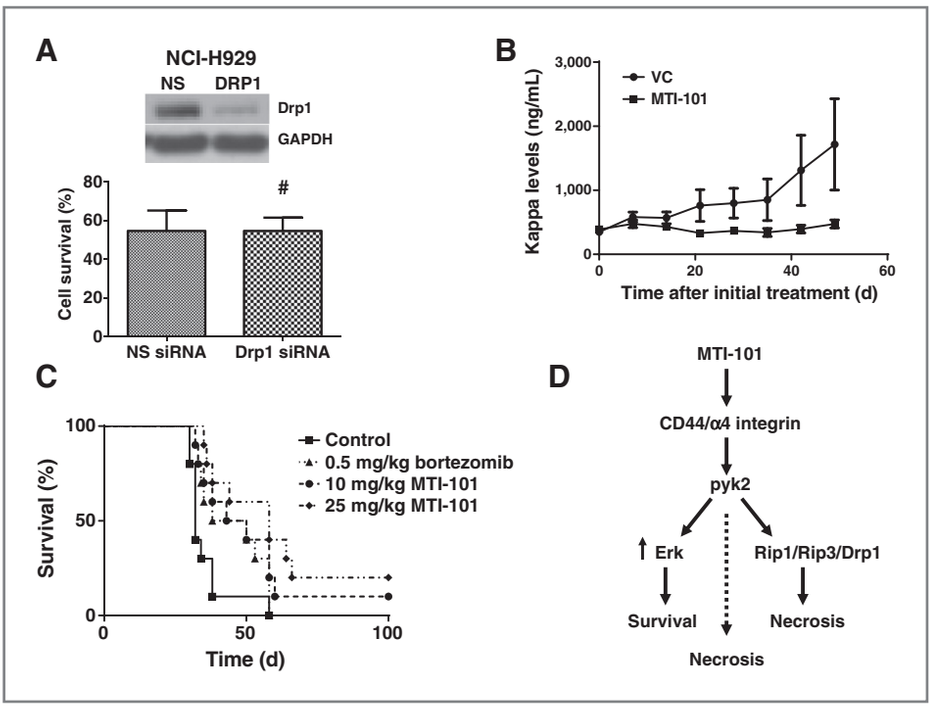


**Figure 6.** MTI-101 has activity as a single agent *in vivo* and MTI-101 necrotic cell death is Drp1 independent in NCI-H929 cell line. A, NCI-H929 cells were incubated with siRNA targeting DRP1 for 72 hours before treatment with 5 μmol/L MTI-101 for 6 hours, and cell death was determined by FACS analysis. NS, nonsilencing. B, in the SCID-Hu model, tumor was allowed to engraft for 28 days and mice were randomized into control and treatment group. On day 28, represented as day 0 on the graph, mice ($N = 10$ for each treatment) were treated intraperitoneally with 8 mg/kg of MTI-101 or PBS daily for 21 days. Tumor burden was assessed weekly by measuring $\kappa$ levels in the sera. MTI-101 treatment demonstrated a significant reduction in tumor burden ($P < 0.05$, ANOVA). C, in the 5TGM1 mouse myeloma model, tumor was allowed to engraft for 10 days and mice ($N = 10$ for each treatment) were treated intraperitoneally at day 10 with agents (MTI-101, bortezomib, or PBS) 3 times a week for 3 weeks. MTI-101 treatment resulted in a significant increase in survival compared with control mice ($P < 0.05$, Mantel–Cox test). Mice were monitored daily for survival with all remaining mice euthanized at day 100 after treatment. D, proposed model of MTI-101 mechanism of action. MTI-101 binds to a CD44 and α4-integrin containing complex, resulting in the recruitment of Pyk2. This complex leads to a pro-survival signal mediated through Erk1/2 and a necrotic cell signal through Rip1/Rip3, and Drp1. There is also a Rip1/Rip3/Drp1 independent pathway that ultimately leads to necrosis. Statistical significance was determined using ANOVA, $P < 0.05$. Knockdown and inhibitor experiments were run in triplicate and repeated 3 times. Statistical significance was determined using Student *t* test, #, $P > 0.05$.

controls (Supplementary Fig. S7). Together these data indicate that MTI-101 is efficacious as a single agent in myeloma *in vivo* model systems and warrants further development for the treatment of myeloma.

## Discussion

Because of the intriguing biological activity of HYD1, we pursued strategies for increasing the therapeutic potential of the linear peptide. These strategies included cyclization of the truncated active core region of HYD1 and alanine scanning substitution, which led to a compound 6- to 10-fold more potent compared to the linear parent peptide *in vitro* as well as demonstrated robust *in vivo* antitumor activity using the SCID-Hu and 5TGM1 myeloma mouse models. Numerous cyclized peptides derived from natural products demonstrate robust bioactivity (36, 37). The therapeutic potential of cyclic peptides is thought to be the result of decreased digestion by proteases as well as constraining the peptide into a confirmation that shares a high affinity for its cognate receptor (38–40). Because of these qualities, peptide cyclization has become an attractive strategy for drug discovery. Certainly, targeting extracellular targets such as integrin–ligand and receptor–ligand interactions is attractive as concerns of poor intracellular accumulation are diminished. A number of cyclized therapeutic agents have shown promise in the clinic, including cyclosporine, numerous antibiotics, and the cyclized RGD integrin binding motif, Cilengitide (41–44). Previously, we demonstrated that HYD1-induced autophagy and caspase-independent necrotic cell death in myeloma cell lines via ATP depletion, ROS production, and depolarization of the mitochondrial membrane potential (14). In this study, we investigated whether the optimized analog MTI-101 would act in a similar manner to the parent compound and found that MTI-101-induced necrotic cell death via similar mechanisms in NCI-H929 and U266 myeloma cell lines. In our present unbiased chemical biology approach using biotinylated HYD1 and LC/MS-MS analysis as an analytical tool for defining the HYD1 binding complex, we identified a number of adhesion receptors,

including α4-, β1-, and β7-integrin, basigin, syndecan, ICAM, NCAM, and CD44, with CD44 abundant in the binding complexes of both NCI-H929 and U266 cell lines. Using an ELISA-based binding assay with full-length recombinant human CD44, we demonstrated that biotin-HYD1 bound to CD44 in a concentration-dependent manner. Furthermore, we replicated this binding with a fluorescently labeled peptide in 8226 cells that overexpressed CD44s. Paradoxically, increased expression of CD44s and subsequent increased binding of the FAM-conjugated peptide did not translate to increased cell death. The observation of increased binding but not increased cell death indicates that expression of CD44 is necessary for binding but may not be sufficient for predicting sensitivity of MTI-101 induced cell death. We speculate that determinants of cell death will likely include a) lateral signaling through VLA-4 integrin b) background signaling of the cell analogous to CD44-dependent depletion of activated T cells and c) expression of CD44 splice variants. Finally, we targeted all isoforms of CD44 using siRNA gene silencing with the goal of assessing its role in MTI-101–induced cell death. Our data indicate that multiple myeloma cell survival is dependent on CD44 expression. To our knowledge, this was the first time that reduced CD44 expression in myeloma cell lines resulted in the activation of cleaved caspase-3. However, this finding was not entirely surprising; as depleting CD44 promoted apoptosis in colon cancer cells (45) as well as it has been reported that CD44 may sequester the Fas receptor (20). Therefore, by reducing CD44 expression, the Fas receptor may become active and induce caspase-dependent cell death. Finally, transient knockdown of other proteins found in the complex such as basigin and syndecan-1 failed to confer resistance to MTI-101–induced cell death. Our finding suggests that CD44 may be an important mediator of cell viability via inhibition of apoptosis and a key regulator of activation of a necrotic cell death in multiple myeloma cells. Together, these observations indicate that CD44 is an excellent candidate to target therapeutically in MM, as is already being done in other cancers (18, 19, 46).

It has been reported that CD44 activation results in the association and activation of Pyk2 during cell adhesion (26–28). Our signaling data indicate that MTI-101 induces a partial agonistic signal as indicated by the formation of a Pyk2–CD44 complex. We did not observe any consistent or robust increase in phosphorylated Pyk2 (data not shown), which may indicate that the peptide induces focal adhesions but does not efficiently drive autophosphorylation and activation of the complex. We also observed activation of the Erk pathway. Activation of the Erk pathway has been reported to be activated by HA binding to CD44 (47), and thus these data are consistent with a partial agonist. Similar results have been obtained with cyclic RGD showing that the peptide can activate αVβ3 signaling as demonstrated by activation of Fak (48). Further studies are required to determine whether MTI-101 competes with binding for known endogenous ligands of CD44 such as fibronectin, ostepontin, or HA. We propose that, understanding the survival signal initiated by MTI-101–induced cell death may lead to rationally designed combination strategies for increasing the efficacy of this novel agent. In this study, we also investigated whether necroptosis was initiated upon MTI-101 treatment. Using siRNA targeting Rip1, Rip3, or Drp1 (critical drivers of necroptosis), we observed a modest, but significant, increase in U266 cell survival upon MTI-101 treatment after reducing the expression of each of these proteins. When we inhibited the canonical necroptotic pathway by using the pharmacological Drp1 inhibitor mdivi-1, we again observed a modest but significant increase in cell survival. Phosphorylated Drp1 levels were also decreased in U266 cells upon MTI-101 treatment. With these same experiments in NCI-H929 myeloma cells, however, we did not observe a statistically significant difference in cell survival upon MTI-101 treatment. Also, mdivi-1 pretreatment failed to protect against MTI-101–induced cell death. We speculate that similar to apoptosis that programmed necrosis is likely regulated by multiple family members and thus contains inherent redundancy. However, genotype differences between H929 and U226 cell lines include an activating BRAF mutation and autocrine interleukin-6 stimulation and constitutive activation of Stat3 in U226 cells. Thus, differences in background genotype may contribute to MTI-101–induced Drp-1–dependent and –independent cell death (49–50). Our work in myeloma cell lines indicates that it will be important to determine the role of MTI-101–induced Drp1-dependent and -independent cell death using primary patient specimens. Our current proposed model indicates that MTI-101 binds a CD44 and α4-integrin containing complex and induces a CD44–Pyk2 complex. This complex activation leads to both a pro-survival signal potentially mediated through Erk1/2 and a necrotic cell signal through Rip1/Rip3 and Drp1. Our data also indicate that we may be activating a novel necrotic cell death pathway that has yet to be fully elucidated and may represent an important pathway for targeting myeloma cells (see Fig. 6D for proposed model of MTI-101–induced cell death and survival signals). Together, these results definitively support continued development of MTI-101 for the treatment of myeloma, providing another therapeutic option for this currently incurable disease.

## Disclosure of Potential Conflicts of Interest

P. Jain is employed as a Senior Research Chemist in Modulation Therapeutics Inc. R.R. Nair is employed as a Senior Scientist in Modulation Therapeutics Inc. R.F. Argilagos is employed as a Research Scientist and has ownership interest (including patents) in Modulation Therapeutics Inc. M.L. McLaughlin is employed as a Executive Vice President and has ownership interest (including patents) in Modulation Therapeutics Inc. L.A. Hazlehurst is employed as a co-founder/president and has ownership interest (including patents) in Modulation Therapeutics Inc. L.A. Hazlehurst also is a consultant/advisory board member of Modulation Therapeutics Inc. No potential conflicts of interest were disclosed by the other authors.

## Authors' Contributions

**Conception and design:** A.W. Gebhard, J.M. Koomen, M.L. McLaughlin, L.A. Hazlehurst
**Development of methodology:** A.W. Gebhard, R.R. Nair, M.F. Emmons, R.F. Argilagos, L.A. Hazlehurst
**Acquisition of data (provided animals, acquired and managed patients, provided facilities, etc.):** A.W. Gebhard, P. Jain, R.R. Nair, M.F. Emmons
**Analysis and interpretation of data (e.g., statistical analysis, biostatistics, computational analysis):** A.W. Gebhard, M.F. Emmons, J.M. Koomen, L.A. Hazlehurst
**Writing, review, and/or revision of the manuscript:** A.W. Gebhard, J.M. Koomen, M.L. McLaughlin, L.A. Hazlehurst
**Administrative, technical, or material support (i.e., reporting or organizing data, constructing databases):** A.W. Gebhard
**Study supervision:** R.R. Nair, M.L. McLaughlin, L.A. Hazlehurst

## Acknowledgments

The authors thank R. Hamilton (Moffitt Cancer Center) for editorial assistance. The authors also thank the Proteomic and Flow Cytometry Core Facilities at H. Lee Moffitt Cancer Center.

## Grant Support

This work was partially funded by NCI 1R01CA122065-01 (L.A. Hazlehurst), Multiple Myeloma Research Foundation Senior Award (L.A. Hazlehurst), and Bankhead-Coley Florida State Grant 2BT03-43424 (L.A. Hazlehurst).

The costs of publication of this article were defrayed in part by the payment of page charges. This article must therefore be hereby marked *advertisement* in accordance with 18 U.S.C. Section 1734 solely to indicate this fact.

Received April 23, 2013; revised August 26, 2013; accepted September 11, 2013; published OnlineFirst September 18, 2013.

## References

1. Kyle RA, Rajkumar SV. Multiple myeloma. N Engl J Med 2004;351:1860–73.
2. Kyle RA, Rajkumar SV. Criteria for diagnosis, staging, risk stratification and response assessment of multiple myeloma. Leukemia 2009;23:3–9.
3. Harousseau JL, Moreau P. Autologous hematopoietic stem-cell transplantation for multiple myeloma. N Engl J Med 2009;360:2645–54.
4. Mihelic R, Kaufman JL, Lonial S. Maintenance therapy in multiple myeloma. Leukemia 2007;21:1150–7.
5. Asosingh K, Gunthert U, De Raeve H, Van Riet I, Van Camp B, Vanderkerken K. A unique pathway in the homing of murine multiple myeloma cells: CD44v10 mediates binding to bone marrow endothelium. Cancer Res 2001;61:2862–5.
6. Azab AK, Runnels JM, Pitsillides C, Moreau AS, Azab F, Leleu X, et al. The CXCR4 inhibitor AMD3100 disrupts the interaction of multiple myeloma cells with the bone marrow microenvironment and enhances their sensitivity to therapy. Blood 2009;113:4341–51.
7. Mori Y, Shimizu N, Dallas M, Niewolna M, Story B, Williams PJ, et al. Anti-alpha4 integrin antibody suppresses the development of multiple myeloma and associated osteoclastic osteolysis. Blood 2004;104:2149–54.
8. Damiano JS, Cress AE, Hazlehurst LA, Shtil AA, Dalton WS. Cell adhesion mediated drug resistance (CAM-DR): role of integrins and resistance to apoptosis in human myeloma cell lines. Blood 1999;93:1658–67.
9. Hazlehurst LA, Damiano JS, Buyuksal I, Pledger WJ, Dalton WS. Adhesion to fibronectin via $\beta$1 integrins regulates p27kip1 levels and contributes to cell adhesion mediated drug resistance (CAM-DR). Oncogene 2000;19:4319–27.
10. Ohwada C, Nakaseko C, Koizumi M, Takeuchi M, Ozawa S, Naito M, et al. CD44 and hyaluronan engagement promotes dexamethasone resistance in human myeloma cells. Eur J Haematol 2008;80:245–50.
11. DeRoock IB, Pennington ME, Sroka TC, Lam KS, Bowden GT, Bair EL, et al. Synthetic peptides inhibit adhesion of human tumor cells to extracellular matrix proteins. Cancer Res 2001;61:3308–13.
12. Pennington ME, Lam KS, Cress AE. The use of a combinatorial library method to isolate human tumor cell adhesion peptides. Mol Divers 1996;2:19–28.
13. Sroka TC, Pennington ME, Cress AE. Synthetic D-amino acid peptide inhibits tumor cell motility on laminin-5. Carcinogenesis 2006;27:1748–57.
14. Nair RR, Emmons MF, Cress AE, Argilagos RF, Lam K, Kerr WT, et al. HYD1-induced increase in reactive oxygen species leads to autophagy and necrotic cell death in multiple myeloma cells. Mol Cancer Ther 2009;8:2441–51.
15. Emmons MF, Gebhard AW, Nair RR, Baz R, McLaughlin M, Cress AE, et al. Acquisition of resistance towards HYD1 correlates with a reduction in cleaved $\alpha$4 integrin expression and a compromised CAM-DR phenotype. Mol Cancer Ther 2011;10:2257–66.
16. Mihalache CC, Yousefi S, Conus S, Villiger PM, Schneider EM, Simon HU. Inflammation-associated autophagy-related programmed necrotic death of human neutrophils characterized by organelle fusion events. J Immunol 2011;186:6532–42.
17. Artus C, Maquarre E, Moubarak RS, Delettre C, Jasmin C, Susin SA, et al. CD44 ligation induces caspase-independent cell death via a novel calpain/AIF pathway in human erythroleukemia cells. Oncogene 2006;25:5741–51.
18. Charrad RS, Gadhoum Z, Qi J, Glachant A, Allouche M, Jasmin C, et al. Effects of anti-CD44 monoclonal antibodies on differentiation and apoptosis of human myeloid leukemia cell lines. Blood 2002;99:290–9.
19. Jin L, Hope KJ, Zhai Q, Smadja-Joffe F, Dick JE. Targeting of CD44 eradicates human acute myeloid leukemic stem cells. Nat Med 2006;12:1167–74.
20. Mielgo A, Brondani V, Landmann L, Glaser-Ruhm A, Erb P, Stupack D, et al. The CD44 standard/ezrin complex regulates Fas-mediated apoptosis in Jurkat cells. Apoptosis 2007;12:2051–61.
21. Dimitroff CJ, Lee JY, Rafii S, Fuhlbrigge RC, Sackstein R. CD44 is a major E-selectin ligand on human hematopoietic progenitor cells. J Cell Biol 2001;153:1277–86.
22. Chen D, McKallip RJ, Zeytun A, Do Y, Lombard C, Robertson JL, et al. CD44-deficient mice exhibit enhanced hepatitis after concanavalin A injection: evidence for involvement of CD44 in activation-induced cell death. J Immunol 2001;166:5889–97.
23. McKallip RJ, Do Y, Fisher MT, Robertson JL, Nagarkatti PS, Nagarkatti M. Role of CD44 in activation-induced cell death: CD44-deficient mice exhibit enhanced T cell response to conventional and superantigens. Int Immunol 2002;14:1015–26.
24. Ruffell B, Johnson P. Hyaluronan induces cell death in activated T cells through CD44. J Immunol 2008;181:7044–54.
25. Siegelman MH, Stanescu D, Estess P. The CD44-initiated pathway of T-cell extravasation uses VLA-4 but not LFA-1 for firm adhesion. J Clin Invest 2000;105:683–91.
26. Li R, Wong N, Jabali MD, Johnson P. CD44-initiated cell spreading induces Pyk2 phosphorylation is mediated by Src family kinases, and is negatively regulated by CD45. J Biol Chem 2001;276:28767–73.
27. Wong NK, Lai JC, Maeshima N, Johnson P. CD44-mediated elongated T cell spreading requires Pyk2 activation by Src family kinases, extracellular calcium, phospholipase C and phosphatidylinositol-3 kinase. Cell Signal 2011;23:812–9.
28. Fujita Y, Kitagawa M, Nakamura S, Azuma K, Ishii G, Higashi M, et al. CD44 signaling through focal adhesion kinase and its anti-apoptotic effect. FEBS Lett 2002;528:101–8.
29. Galluzzi L, Kroemer G. Necroptosis: a specialized pathway of programmed necrosis. Cell 2008;135:1161–3.
30. Vandenabeele P, Galluzzi L, Vanden Berghe T, Kroemer G. Molecular mechanisms of necroptosis: an ordered cellular explosion. Nat Rev Mol Cell Biol 2010;11:700–14.
31. Cassidy-Stone A, Chipuk JE, Ingerman E, Song C, Yoo C, Kuwana T, et al. Chemical inhibition of the mitochondrial division dynamin reveals its role in Bax/Bak-dependent mitochondrial outer membrane permeabilization. Dev Cell 2008;14:193–204.

32. Sun L, Wang H, Wang Z, He S, Chen S, Liao D, et al. Mixed lineage kinase domain-like protein mediates necrosis signaling downstream of RIP3 kinase. Cell 2012;148:213–27.
33. Wang Z, Jiang H, Chen S, Du F, Wang X. The mitochondrial phosphatase PGAM5 functions at the convergence point of multiple necrotic death pathways. Cell 2012;148:228–43.
34. Urashima M, Chen BP, Chen S, Pinkus GS, Bronson RT, Dedera DA, et al. The development of a model for the homing of multiple myeloma cells to human bone marrow. Blood 1997;90:754–65.
35. Yaccoby S, Barlogie B, Epstein J. Primary myeloma cells growing in SCID-Hu mice: a model for studying the biology and treatment of myeloma and its manifestations. Blood 1998;92:2908–13.
36. Joullie MM, Richard DJ. Cyclopeptide alkaloids: chemistry and biology. Chem Commun (Camb) 2004:2011–5. [Epub 2004 Aug 31]
37. Sainis I, Fokas D, Vareli K, Tzakos AG, Kounnis V, Briasoulis E. Cyanobacterial cyclopeptides as lead compounds to novel targeted cancer drugs. Mar Drugs 2010;8:629–57.
38. Rew Y, Malkmus S, Svensson C, Yaksh TL, Chung NN, Schiller PW, et al. Synthesis and biological activities of cyclic lanthionine enkephalin analogues: Δ-opioid receptor selective ligands. J Med Chem 2002; 45:3746–54.
39. Davies JS. The cyclization of peptides and depsipeptides. J Peptide Sci 2003;9:471–501.
40. Craik DJ, Cemazar M, Daly NL. The cyclotides and related macrocyclic peptides as scaffolds in drug design. Curr Opin Drug Discov Develop 2006;9:251–60.
41. Tedesco D, Haragsim L. Cyclosporine: a review. J Transplant 2012; 2012:230386.
42. Nagarajan M, Maruthanayagam V, Sundararaman M. A review of pharmacological and toxicological potentials of marine cyanobacterial metabolites. J Appl Toxicol 2012;32:153–85.
43. Scaringi C, Minniti G, Caporello P, Enrici RM. Integrin inhibitor cilengitide for the treatment of glioblastoma: a brief overview of current clinical results. Anticancer Res 2012;32:4213–23.
44. Mas-Moruno C, Rechenmacher F, Kessler H. Cilengitide: the first anti-angiogenic small molecule drug candidate design, synthesis and clinical evaluation. Anticancer Agents Med Chem 2010;10:753–68.
45. Park Y, Huh J, Lee J, Kim H. shRNA against CD44 inhibits cell proliferation, invasion and migration, and promotes apoptosis of colon cancer carcinoma cells. Oncol Rep 2012;27:339–46.
46. Riechelmann H, Sauter A, Golze W, Hanft G, Schroen C, Hoermann K, et al. Phase I trial with the CD44v6-targeting immunoconjugate bivatuzumab mertansine in head and neck squamous cell carcinoma. Oral Oncol 2008;44:823–9.
47. Meran S, Luo DD, Simpson R, Martin J, Wells A, Steadman R, et al. Hyaluronan facilitates transforming growth factor-beta1-dependent proliferation via CD44 and epidermal growth factor receptor interaction. J Biol Chem 2011;286:17618–30.
48. Alghisi GC, Ponsonnet L, Ruegg C. The integrin antagonist cilengitide activates $\alpha V\beta 3$, disrupts VE-cadherin localization at cell junctions and enhances permeability in endothelial cells. PLoS One 2009;4:e4449.
49. Catlett-Falcone R, Landowski TH, Oshiro MM, Turkson J, Levitzki A, Savino R, et al. Constitutive activation of Stat3 signaling confers resistance to apoptosis in human U266 myeloma cells. Immunity 1999;10:105–15.
50. Ng MH, Lau KM, Wong WS, To KW, Cheng SH, Tsang KS, et al. Alterations of RAS signalling in Chinese multiple myeloma patients: absent BRAF and rare RAS mutations, but frequent inactivation of RASSF1A by transcriptional silencing or expression of a non-functional variant transcript. Br J Haematol 2003;123: 637–45.